

# ForensicTransfer: Weakly-supervised Domain Adaptation for Forgery Detection

Davide Cozzolino<sup>1</sup> Justus Thies<sup>2</sup> Andreas Rössler<sup>2</sup> Christian Riess<sup>3</sup>  
 Matthias Nießner<sup>2</sup> Luisa Verdoliva<sup>1</sup>

<sup>1</sup>University Federico II of Naples <sup>2</sup>Technical University of Munich  
<sup>3</sup>University of Erlangen-Nuremberg

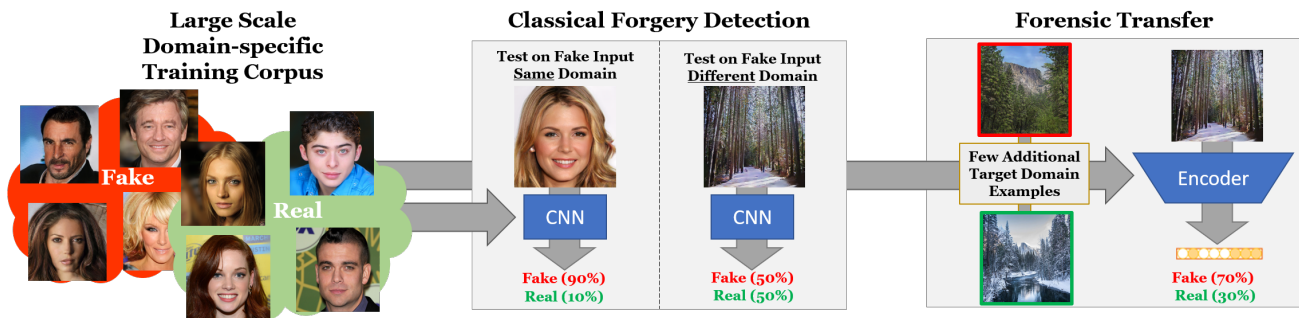


Figure 1: CNN-based approaches for image forgery detection tend to overfit to the source training data and perform bad on new unseen manipulations. *ForensicTransfer* introduces a new autoencoder-based architecture that is able to overcome this problem given only few labeled target examples. The idea is to learn a discriminative feature representation in the latent space so that only specific components of the hidden vector are activated for the pristine and forged classes.

## Abstract

Distinguishing fakes from real images is becoming increasingly difficult as new sophisticated image manipulation approaches come out by the day. Convolutional neural networks (CNN) show excellent performance in detecting image manipulations when they are trained on a specific forgery method. However, on examples from unseen manipulation approaches, their performance drops significantly. To address this limitation in transferability, we introduce *ForensicTransfer* (FT). *ForensicTransfer* tackles two challenges in multimedia forensics. First, we devise a learning-based forensic detector which adapts well to new domains, i.e., novel manipulation methods. Second we handle scenarios where only a handful of fake examples are available during training. To this end, we learn a forensic embedding that can be used to distinguish between real and fake imagery. We are using a new autoencoder-based architecture which enforces activations in different parts of a latent vector for the real and fake classes. Together with the constraint of correct reconstruction this ensures that the latent

space keeps all the relevant information about the nature of the image. Therefore, the learned embedding acts as a form of anomaly detector; namely, an image manipulated from an unseen method will be detected as fake provided it maps sufficiently far away from the cluster of real images. Comparing with prior works, FT shows significant improvements in transferability, which we demonstrate in a series of experiments on cutting-edge benchmarks. For instance, on unseen examples, we achieve up to 80-85% in terms of accuracy compared to 50-59%, and with only a handful of seen examples, our performance already reaches around 95%.

## 1. Introduction

Image manipulation is as old as photography itself [15]; however, with recent advances in machine learning and synthetic image rendering, it has reached unprecedented levels of diffusion and sophistication. Manipulations that were once possible only for high-budget movie productions are now within the reach of anyone who can access large

amounts of data — a democratization of high quality image and video synthesis. This development is the outcome of intense research in computer vision, driven by market demands in the movie industry, photography, virtual reality, game playing, and autonomous driving. A major focus of research has been face synthesis and manipulation. Nowadays, we can generate entirely synthetic faces [9, 24], even at very high-resolutions [22], animate a subject’s face to make it express the desired emotions [5, 31], or modify facial expressions [39, 37, 23]. Beyond faces, a number of generic image manipulation methods have been proposed. It is now possible to transfer semantic content from a source domain to a target domain characterized by a different style [45], create automatically image compositions [46], and reconstruct missing image parts by semantic inpainting [26, 21]. It is worth noting that most of these operations can be carried out using several editing tools (e.g., *Photoshop*, *GIMP*), and with some manual effort achieve highly convincing results.

Although these processing tools were originally designed for benign applications, they can also be used to perform high-quality image forgeries. Realistic fake content can have a high impact on people’s life, as demonstrated by the *Deepfake app* [1]. They can be used to support fake news, and cause their viral spread over ubiquitous social networks. Therefore, it is critical to develop methods that allow the reliable detection of such manipulations, and there has been growing attention towards this goal in the research community. Deep neural networks have proven to be very effective for this task and several works can be found in the current literature [7, 11, 32, 34, 3]. However, such techniques turn out to be highly manipulation-specific. I.e., they perform very well for the manipulation they were trained on, but they provide disappointing results on images created with unseen manipulation methods, even though they are semantically close. We speculate that the underlying neural networks quickly overfit to manipulation-specific artifacts, thus learning features that are highly discriminatory for the given task but severely lack transferability. This lack of transferability is a major weakness of current learning-based approaches for forensics. It can be partially addressed by fine-tuning a pre-trained net with new task-specific data, but this means that new large amounts of data are necessary. Due to the high dynamics in the field of digital content synthesis this is not feasible and introduces a huge time delay for every new method that has to be debunked. Ideally, one would like to detect a forgery even if the network has not been trained for it, or if only a few labeled examples are available. The goal of this work is to develop a CNN-based method that ensures such generalization; i.e., being able to transfer knowledge between different but related manipulations. To the best of our knowledge, this is the first work addressing this problem in the context of multimedia foren-

sics. To this end, we make the following contributions:

- We introduce a novel autoencoder-based neural network architecture, that learns a model for a derived embedding capable of transferring between different manipulation domains.
- We show that this transferability enables robust forgery detection even when no or only a handful of training samples of a new manipulation method is available.
- In comparison to the baselines, our accuracy increases by 10% (using less than four samples for the target manipulation).

## 2. Related work

While the main focus of our work lies in the field of media forensics, *ForensicTransfer* also intersects with the field of transfer learning. There is a wide range of image forgery detection methods. These methods can be divided into traditional model-based and learning-based approaches.

**Traditional Media Forensics** Traditional model-based approaches exploit a specific clue, like inconsistencies at pixel-level related for example to JPEG compression artifacts [4], demosaicking clues [16], lens aberration [41], or camera noise [29]. They are very effective, but also very sensitive to the assumed hypotheses. Robustness is much more ensured by physics-based approaches that rely on inconsistencies in illumination or perspective mappings [14]; however, they are still not able to provide a performance comparable to pixel-based methods in realistic situations.

**Learned Media Forensics** Recently, the research community has shown that supervised deep learning approaches can achieve impressive detection results. To this end, several different architectures have been proposed the last few years. The first ones force the network to work on noise residuals by suppressing the scene content, given that most significant artifacts are hidden in the high-pass filtered version of the signal. This can be accomplished by adding a first layer of fixed high-pass filters [33, 27], learned filters [7], or even by recasting hand-crafted features working on residuals as a convolutional neural network (CNN) [11]. In [44] a two-stream network is proposed that exploits both low-level and high-level features. A first network is constrained to work on noise residuals while the second one is a general purpose deep CNN. Other architectures try to exploit even possible boundary artifacts created by the editing process when for example an object is spliced into the image [36, 6].

A significant performance gap can be observed by very deep networks especially on compressed data [34], which

is an important feature to detect fake content on social networks. However, all proposed learning-based methods need some form of finetuning on a dataset that comprises manipulations aligned with the ones present in the test set. E.g., a common form of polarization is present when a limited number of cameras is used to create the data in the training and test set. In fact, even if different images are used for training and testing, the same camera-based artifacts are present in the background of the image, making the whole learning procedure flawed. To avoid any form of polarization on the training-set, recent approaches have adopted Siamese networks to train couples of patches [20, 12]. This way, they do not need to rely on a specific training set, since they are acting as anomaly detectors on a pixel-level basis. Hence, their performance are much more effective on localization than on detection.

Most of the approaches present in the current literature are devoted to detect classical manipulations, i.e., modifications carried out using basic low-level operations, like compositions, clones, or removals of areas through exemplar-based inpainting. Fewer works [30, 3] instead address the problem of detecting more recent form of manipulations, that use advanced computer graphics tools or artificial intelligence. In addition, these approaches operate always in a supervised setting, where one can rely on a training set comprising data modified exactly with the same algorithm. In contrast to these methods, we are not restricted to a specific type of manipulation and only need a few samples to adapt to new manipulations.

**Transfer learning** Transfer learning is an important problem in the vision community, especially, in deep learning which relies on a large amount of training data compared to traditional machine learning approaches. Hence, several solutions have been proposed to adapt the source domain to the target domain in different scenarios [13]. Another direction is to learn a latent embedding in the source domain from which the feature space in the target domain is derived [17, 8]. In the Zero Shot or Few Shot Learning scenario, the use of autoencoders as tools to learn a better semantic representation has been also explored in [25]. Recently, generative adversarial networks (GANs) have been also used [18] in order to bridge the gap between two different (but similar) domains [19, 40].

### 3. Problem Statement

*ForensicTransfer* tackles the problem of detecting novel unseen manipulation methods, without the need of a large amount of training data. To this end, we introduce a CNN-based forensic detector that transfers to new forensic scenarios, i.e., with no or only very few samples in the target domain (see Sec. 4).



Figure 2: Two examples of images manipulated with Face2Face [39] and FaceSwap [2] (left) and their corresponding class activation maps, when the network (XceptionNet [10]) is trained on Face2Face forgeries (middle) and when it is trained on FaceSwap ones (right).

Specifically, we train a classifier on a database of manipulated images (source domain) and transfer the domain knowledge to a different target domain that contains images of another manipulation method. We assume a large dataset for the source domain and only few or no images from the target domain.

As known from the literature, based on a large dataset, a classifier can be trained to detect test images from the source domain with a satisfactory performance. However, we would also like the classifier to detect images from the target domain. This is of paramount importance in a real-world scenario, since new manipulation methods appear day by day, and retraining a domain-specific classifier may be impractical or simply impossible due to the lack of labeled data. As reviewed in the related work section, existing CNN-based detectors lack this ability to transfer between domains, even if they are closely related. To showcase this problem, we trained XceptionNet [10] on images generated by Face2Face [39], which achieves an accuracy of 98.13%. A similar performance is achieved when the

network is trained to detect images generated by FaceSwap [2], achieving an accuracy of 98.30%. In Fig. 2, we show two examples of class activation maps (CAMs), obtained using the approach proposed by [43], for the same subject manipulated with the two approaches. They clearly show that the network learns to focus on some specific features based on the type of forgery. As an undesired consequence, a forged image which lacks these artifacts may escape the detector scrutiny. This becomes problematic when we swap the test sets: now, we train on Face2Face and test on FaceSwap and vice-versa. Thus, train and test sets are generated from different (even though related) approaches. Therefore, the cross-domain accuracies drop to 50.20% and 52.73%, respectively – this is only marginally better than random chance.

In the following section, we show how we address these shortcomings and introduce a CNN-based detector which is as good as conventional detectors when trained on method-A images (source domain), but also learns to detect method-B images (target domain) with only a few or no sample images. Sec. 5 gives a thorough analysis of our approach and comparisons to state-of-the-art methods.

## 4. Proposed Method

The idea of our method is to disentangle the knowledge that we can gain from training on a source domain into the knowledge about fake and real imagery. To this end, we designed an encoder-decoder network, where we specifically force the latent space to be partitioned into two parts. One part exclusively for real and the other part exclusively for the fake samples. Since the network has to reproduce the image content, all information about the input has to be stored in the latent space. Thus, these features of the learned forensic embedding are rich and contain general information of an image. And can be used to distinguish between fake and real imagery by measuring the activation in the different parts.

**Forensic Embedding:** Given an input image  $x_i$  we apply the encoder function  $\mathcal{E}(\cdot)$  (see Sec. 4.1) to derive the latent space vector  $h_i$ :

$$\mathcal{E}(x_i) = h_i = \{h_{i,0}, h_{i,1}\} . \quad (1)$$

We split the latent space vector in two disjunct parts,  $h_{i,0}$  and  $h_{i,1}$ . In particular, the encoder  $\mathcal{E}(x_i)$  is trained to activate  $h_{i,0}$  if and only if  $x_i$  is a sample of the real images and  $h_{i,1}$  otherwise.

**Disentangling Loss:** To enforce the disentangling of the two classes (fake and real) in the latent space  $h_i$ , we are using a loss function that combines both, a reconstruction

loss  $\mathcal{L}_{REC}$  and a activation loss  $\mathcal{L}_{ACT}$ :

$$\mathcal{L} = \mathcal{L}_{ACT} + \gamma \cdot \mathcal{L}_{REC} . \quad (2)$$

$\gamma$  weights the influence of the reconstruction error and is set to 0.1 for all our experiments. We are using the commonly used  $\ell_1$ -loss as reconstruction metric:

$$\mathcal{L}_{REC} = \frac{1}{N} \sum_i \|x_i - \hat{x}_i\|_1 , \quad (3)$$

given  $N$  the number of element of input images  $x_i$  and the reconstruction  $\hat{x}_i = \mathcal{D}(h_i)$ . Where  $\mathcal{D}(\cdot)$  denotes the decoder network.

The activation loss measures the activation of the latent space vector  $h_i$  w.r.t. the given label  $l_i$ :

$$\mathcal{L}_{ACT} = \sum_i |a_{i,1} - l_i| + |a_{i,0} - (1-l_i)| \quad (4)$$

Here,  $a_{i,c}$  computes the per class activation of the latent space and is defined as:

$$a_{i,c} = \frac{1}{K_c} \|h_{i,c}\|_1 \quad c \in \{0,1\} , \quad (5)$$

where  $K_c$  is the number of features of  $h_{i,c}$ . The activation loss ensures that for a given sample  $x_i$  of class  $c$ , the corresponding part of the latent space  $h_{i,c}$  to be active, with at least one non zero element, thus,  $a_{i,c} > 0$ . On the contrary, the off-class part of the latent space  $h_{i,1-c}$  has to be silent, i.e.,  $a_{i,1-c} = 0$ .

**Classification:** During test time, the forgery detection is based on the activation of the latent space partitions. A sample  $x_i$  is considered to be fake ( $c = 1$ ) if  $a_{i,1} > a_{i,0}$ , and real otherwise.

**Transferability:** Given a new image from a target domain, one can use the encoder of the source domain to determine the forensic embedding. Based on the classification rule mentioned in the previous paragraph, we are able to decide whether the input is closer to the real or to the fake images of the source domain. If the two manipulation methods share specific artifacts, a fake image of the target domain is closer to the fake images of the source domain. Given a few samples of the target domain we are able to fine-tune the classifier, as we can show in Sec. 5.

To get a sense of the transferability of our proposal, we compare the results using our novel approach to the experiment described in Sec. 3 by visualizing the class activation maps (see Fig. 3, cp. to Fig. 2). In contrast to a deep CNN like XceptionNet, our approach is able to adapt to the different artifacts of Face2Face and FaceSwap (the nose in the first case, the eyebrows and mouth in the second case). Fine-tuning on few images further helps to rely on these different artifacts.



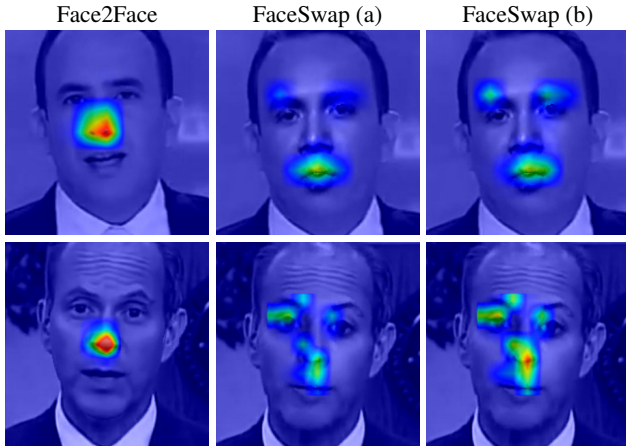


Figure 3: Class activation maps for our method when it is trained on Face2Face [39] and tested on Face2Face forgeries (left) or FaceSwap [2] (middle), and finally trained on Face2Face but fine-tuned using only four images manipulated with FaceSwap and tested on FaceSwap (right).

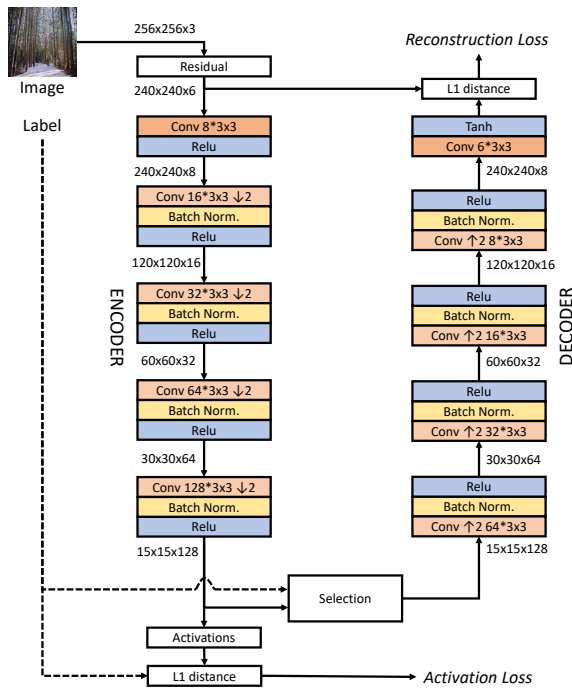


Figure 4: *ForensicTransfer* neural network architecture. As input we take an image from which we first derive the residual image, which is then fed into an encoder (left). The learned embedding is constrained by the activations of the class loss (fake vs real), as well as the reconstruction loss of the decoder (right).

## 4.1. Network architecture

In this work we consider an encoder-decoder architecture shown in Fig.4. Input images have a size of  $256 \times 256$  or  $128 \times 128$  pixels, depending on the dataset (see Sec. 5). The encoder and decoder have mirrored structures, with 5 convolutional layers each, and without skip connections. In the encoder, all convolutions, except the first one, have stride 2, reducing spatial resolution by a factor 16. To recover the original size, the decoder employs a  $2 \times 2$  nearest-neighbor up-sampling before each convolution (except the last one). All activation functions are ReLUs (Rectified Linear Units), except for the hyperbolic tangent activation used in the last layer to ensure the output to be in the range of  $[-1, 1]$ . The latent space at the encoder output, has 128 feature maps, 64 associated with the class 'real' and 64 with the class 'fake'. Activations are measured as defined in equation 5. The selection block sets the off-class part of latent space to zero, depending on the class label, forcing the decoder to learn how to reconstruct the input sample only from the same-class part of the latent space.

We also evaluate a variant of this architecture (FT-res). It is well-known in multimedia forensics that the most valuable information for forgery detection is in the high-pass image content. Thus, we extract so called residual images by applying a high-pass filter to the images. In particular, we apply a third-order derivative as done in [11] along the vertical and horizontal direction for each color band to compute the residual image. These residual images are then used as input to our method.

## 4.2. Training

To evaluate its generalization capability, the network is first accurately trained on a dataset built w.r.t. a specific manipulation method (source domain). We are then fine-tuning the network on few images subject to a different (but similar) manipulation class (target domain). The fine-tuning procedure enables us to quickly adapt our detection network to new manipulation scenarios without the need of re-training the whole network.

For training, we use the ADAM gradient-based optimization scheme with a learning rate of 0.001, a batch-size of 64 and default values for the moments ( $\beta_1 = 0.9$ ,  $\beta_2 = 0.999$  and  $\epsilon = 10^{-7}$ ). We train the network until the loss, evaluated on the validation, does not improve for 30 consecutive epochs.

## 5. Results

In this section we give a thorough analysis of our novel approach to detect image forgeries. To this end, we are using multiple datasets of different manipulation techniques (see Sec. 5.1) and show state-of-the-art detection results in comparison to previous methods (see Sec. 5.2).



Figure 5: Examples of GAN generated images. Left: real faces coming from CelebA-HQ dataset [22] compared with synthetic faces generated by Progressive-GAN [22]. Right: real images compared with their fake versions generated by Cycle-GAN using [45].

### 5.1. Datasets

In our experiments we focus on manipulations performed by computer graphics (CG) or deep learning methods, which may involve parts of real images (for example, changes in the mouth to follow a desired text) or the generation of whole synthetic images. In all cases, we used large datasets for the source domain. Each dataset is split in training, validation and test, guaranteeing that the same pristine images are present for related but different manipulations. The few examples of the target dataset, used for fine-tuning, are randomly extracted from the training and validation sets. Note that we took care to pair two different but related manipulations in all our experiments for the source and target dataset. In the following we describe each dataset.

**Synthetic images:** Because of the lack of publicly available dataset for forensic research purposes, we built 4 datasets of 30000 images each comprising images generated using progressive GAN [22], Cycle-GAN [45], Glow [24], and StarGAN [9]. Progressive GAN generates high resolution faces, Cycle-GAN performs image-to-image translation (see Fig.5), and the last two methods change attributes of a face (see Fig.6). Except for the high resolution images of dimension  $1024 \times 1024$ , all the other output images are  $256 \times 256$  pixels.

The total number of 30000 images per manipulation method is split into 21000, 6000 and 3000 image set for training, validation and test, respectively. For our test we used the progressive GAN and StarGAN images as the source datasets while Cycle-GAN and Glow are chosen to be the target datasets, respectively.

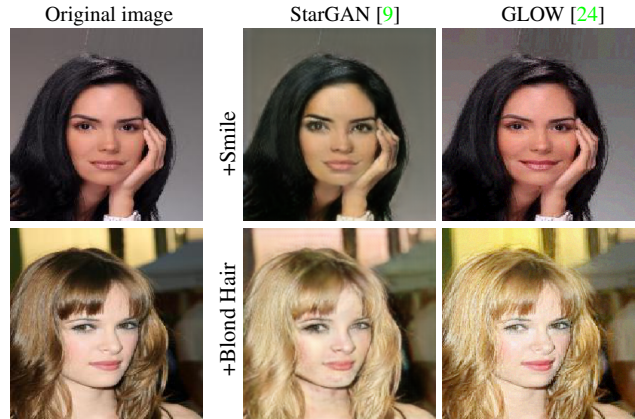


Figure 6: Examples of GAN-based attribute modification. Real images coming from CelebA dataset [28] (left) and their fake versions generated by StarGAN [9] and Glow [24] using the same attributes.

**Inpainted images:** We built another two datasets of 20000 images each using inpainting-based manipulation methods. To this end, we created a source database using the method of Iizuka et al. [21] and a target database using Yu et al. [42]. Some examples are shown in Fig.7. The inpainting is applied to the central  $128 \times 128$ -pixel region of the image. The manipulated image is compressed in JPEG format with the same quality parameter of the relative original image [35]. Since only the central region is manipulated, we considered only this part as the input for the networks. The set of 20000 images are split into 14000, 3000, 3000 images for training, validation and test, respectively.

**CG-based manipulated faces:** We are using the public dataset *FaceForensics*, proposed in [34], with 1004 real videos and 1004 fake ones manipulated by *Face2Face* [39]. We used the same original videos to create another dataset of manipulated videos using *FaceSwap* [2]. The *Face2Face* generated images are used as the source dataset and the *FaceSwap* manipulation as the target dataset. The 1004 videos are divided into 704 for training, 150 for validation and 150 for testing. All videos have been compressed using H.264 with quantization parameter set to 23. During the training we used 200 frames from each video, while the testing is performed on ten frames per video. For each frame, we cropped all images to be centered around the face. Some examples of such images are shown in Fig.8.

### 5.2. Comparison to State-of-the-art

In this section we are comparing our method to several state-of-the-art CNN-based detection methods. Bayar16 [7] and Cozzolino17 [11] have been proposed to detect generic manipulations based on a constrained net-

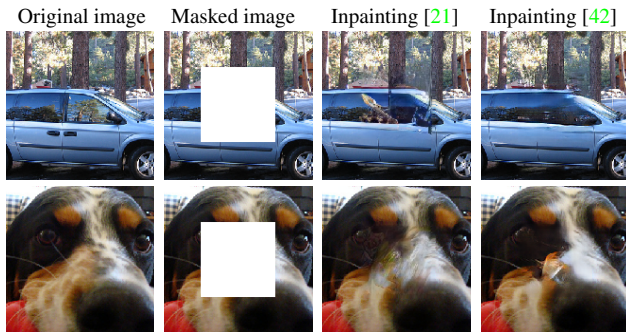


Figure 7: Examples of inpainting-based manipulations. The original images come from ImageNet [35], the central  $128 \times 128$ -pixel region is inpainted by the methods proposed in [21] and [42].



Figure 8: Examples of CG-based manipulated faces. From left to right: original frame, face manipulated using Face2Face [39] and FaceSwap [2]. Original videos and Face2Face ones are of the FaceForensics dataset [34]. The FaceSwap videos are created from the same original videos.

work. Rahmouni17 [32] detects computer-generated images, while MesoInception-4 was proposed [3] for deepfake detection. We are also considering a general-purpose state-of-the-art deep network, XceptionNet [10], given the excellent performance shown in [34] for facial manipulation detection.

In the following, we briefly describe these baseline methods:

*Bayar16* [7]: is a constrained network that uses a convolutional layer designed to suppress the high-level content of the image (total of 8 layers).

*Cozzolino17* [11]: is a CNN-based network that rebuilds hand-crafted features used in the forensic community. These features are extracted as co-occurrences on 4 pixels patterns along the horizontal and vertical direction on the residual image, obtained after high-pass filtering the input data.

*Rahmouni17* [32]: integrates the computation of statistical feature extraction within a CNN framework. We adopt

the best performing network (Stats-2L).

*MesoInception-4* [3]: is a CNN-based network proposed to detect *DeepFakes*. The network includes inception modules inspired by InceptionNet [38]. During training, the mean squared error between true and predicted labels is used as loss instead of the classic cross-entropy loss.

*XceptionNet* [10]: is based on depth-wise separable convolution layers with residual connections. XceptionNet is pre-trained on ImageNet.

To ensure fairness, all methods are trained exactly on the same dataset as specified in the previous Section. When necessary, images have been rescaled [10, 3] or clipped [7, 11, 32], to match the size of the network input layer as specified in the original papers.

**Generalization Analysis:** First of all, we evaluate the ability of each network to detect a manipulation performed with the same method seen in the training set (source) and with a different method (target) *without any form of fine-tuning*. This experiment is important to understand the intrinsic transferability of a network. We paired the datasets described in Sec. 5.1 to consider similar types of manipulations.

The results are listed in Tab. 1. On the source domain, all methods, including the proposed ones, perform very well, with accuracies close to 100%, which lower only on the video datasets, where frames are subject to a much stronger compression than images of the other datasets. In the case of compression, *XceptionNet* exhibits a superior performance, as already observed in [34]. When evaluating the trained networks on the respective target domain, we observe a dramatic performance loss for all reference methods, most of which provide accuracies close to 50% (coin tossing). These results prove a scarce generalization ability for deep learning-based methods, and motivate our efforts to improve under this respect. Partial exceptions are represented by Cozzolino17, on the inpainting and video datasets, and Rahmouni17, only on videos. *ForensicTransfer* also shows a performance impairment; however, the residual-based network maintains good performance; e.g., 85% accuracy from Pro.GAN [22] to CycleGAN [45].

**Adaptation Analysis:** In our adaptation experiment we measure the ability of the baseline methods and our proposed networks to adapt to the target domain using a limited number of labeled examples. In Fig. 12 we show accuracies as a function of the number of images of training for fine-tuning, ranging from 1 to 100, randomly selected from the whole training set of target dataset. During the fine-tuning, we also use a small validation set equal to three-fifths of the small training set. Curves start from zero-shot values as discussed in the generalization paragraph. For all reference methods, the accuracy grows quite slowly with fine-tuning



	Pro.GAN [22] vs CycleGAN [45]		StarGAN [9] vs Glow [24]		Inpainting [21] vs Inpainting [42]		Face2Face [39] vs FaceSwap [2]	
	Source	Target	Source	Target	Source	Target	Source	Target
Bayar16 [7]	99.92	50.42	99.98	50.00	99.08	50.10	92.93	52.87
Cozzolino17 [11]	99.92	52.43	100.0	50.00	98.12	63.33	79.80	<b>77.77</b>
Rahmouni17 [32]	100.0	49.87	100.0	50.00	95.35	52.02	93.57	70.87
MesoInception-4 [3]	97.47	44.19	99.50	49.97	87.65	67.30	85.87	45.17
XceptionNet [10]	100.0	58.79	100.0	50.00	<b>99.98</b>	51.08	<b>98.13</b>	50.20
FT (ours)	100.0	51.48	100.0	54.30	99.92	50.10	94.17	70.23
FT-res (ours)	<b>100.0</b>	<b>85.00</b>	<b>100.0</b>	<b>82.05</b>	99.77	<b>70.62</b>	94.47	72.57

Table 1: Accuracy on the Source dataset and Target dataset. All the methods perform very well on the manipulations seen in the training set and much worse on new ones.

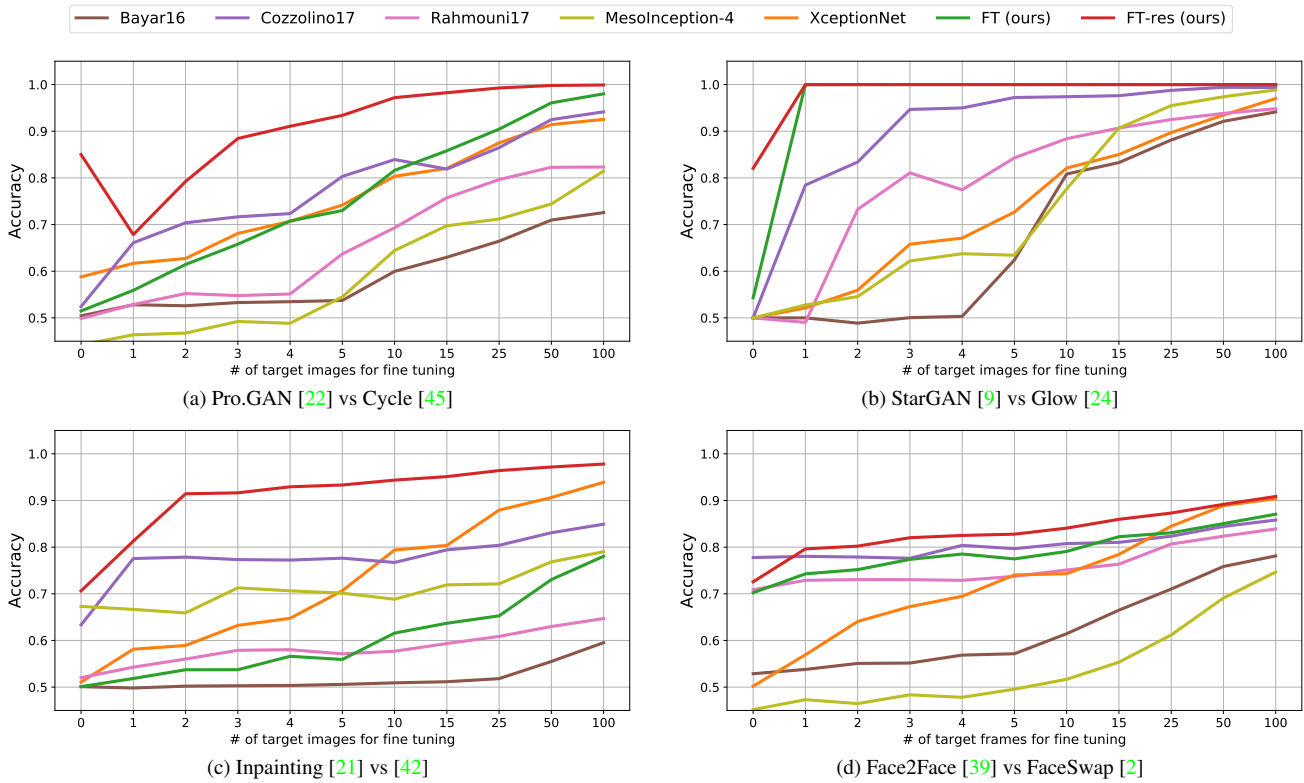


Figure 9: Few-shot adaptation. Plots show accuracy versus number of images used for fine-tuning (shots). Values are averaged over 10 runs. Note the zero and few-shot transferability of *ForensicTransfer* (FT-res, red curves).

(note the non-uniform sampling of the  $x$ -axis) and in many cases remains largely below 100% even at 100 training images. *ForensicTransfer*, instead, reaches a very high accuracy with just a few shots, and outperforms all competitors with a large margin. On the Pro.GAN-CycleGAN dataset, the accuracy exceeds 90% at 4 shots, and reaches 100% before 100 sample images. On StarGAN-Glow results are impressive and one shot is already enough. On the inpainting dataset, the 90% mark is reached with two shots, and almost

100% using 100 training images. Only for the more challenging Face2Face-FaceSwap experiment, a slower growth and a smaller gain is observed, with XceptionNet almost closing the gap at 100 shots, both with accuracy exceeding 90%.



## 6. Conclusion

We introduce *ForensicTransfer* a new method to facilitate transferability between image manipulation domains. Specifically, we address the shortcomings of convolutional neural networks that when trained for a given manipulation approach, are unable to achieve good detection results on different edits – even when they are related. In comparison to traditional learning techniques, we can achieve significantly higher detection rates in cases where no or only a few training samples are available in the target domain. Overall, we believe that our method is a stepping stone towards forgery detectors that only need a few training samples of the target domain.

## 7. Acknowledgement

We gratefully acknowledge the support of this research by the AI Foundation, a TUM-IAS Rudolf Mößbauer Fellowship, and Google Faculty Award. In addition, this material is based on research sponsored by the Air Force Research Laboratory and the Defense Advanced Research Projects Agency under agreement number FA8750-16-2-0204. The U.S. Government is authorized to reproduce and distribute reprints for Governmental purposes notwithstanding any copyright notation thereon. The views and conclusions contained herein are those of the authors and should not be interpreted as necessarily representing the official policies or endorsements, either expressed or implied, of the Air Force Research Laboratory and the Defense Advanced Research Projects Agency or the U.S. Government.

## References

- [1] Deepfake. <https://www.deepfakes.club/openfaceswap-deepfakes-software/>. 2
- [2] Faceswap. <https://github.com/MarekKowalski/FaceSwap/>. 3, 5, 6, 7, 8
- [3] D. Afchar, V. Nozick, J. Yamagishi, and I. Echizen. MesoNet: a compact facial video forgery detection network. In *IEEE International Workshop on Information Forensics and Security (WIFS)*, 2018. 2, 3, 7, 8, 12
- [4] S. Agarwal and H. Farid. Photo Forensics from JPEG Dimples. In *IEEE International Workshop on Information Forensics and Security (WIFS)*, 2017. 2
- [5] H. Averbuch-Elor, D. Cohen-Or, J. Kopf, and M. F. Cohen. Bringing portraits to life. *ACM Transactions on Graphics (Proceeding of SIGGRAPH Asia 2017)*, 36(4):to appear, 2017. 2
- [6] J. Bappy, A. Roy-Chowdhury, J. Bunk, L. Nataraj, and B. Manjunath. Exploiting spatial structure for localizing manipulated image regions. In *Computer Vision and Pattern Recognition Workshops*, pages 4970–4979, 2017. 2
- [7] B. Bayar and M. Stamm. A deep learning approach to universal image manipulation detection using a new convolutional layer. In *ACM Workshop on Information Hiding and Multimedia Security*, pages 5–10, 2016. 2, 6, 7, 8, 12
- [8] M. Chen, Z. Xu, K. Weinberger, and F. Sha. Marginalized denoising autoencoders for domain adaptation. In *International Conference on Machine Learning*, pages 1627–1634, 2012. 3
- [9] Y. Choi, M. Choi, M. Kim, J.-W. Ha, S. Kim, and J. Choo. StarGAN: Unified Generative Adversarial Networks for Multi-Domain Image-to-Image Translation. In *IEEE Conference on Computer Vision and Pattern Recognition (CVPR)*, 2018. 2, 6, 8, 11
- [10] F. Chollet. Xception: Deep Learning with Depthwise Separable Convolutions. In *IEEE Conference on Computer Vision and Pattern Recognition (CVPR)*, 2017. 3, 7, 8, 12
- [11] D. Cozzolino, G. Poggi, and L. Verdoliva. Recasting residual-based local descriptors as convolutional neural networks: an application to image forgery detection. In *ACM Workshop on Information Hiding and Multimedia Security*, pages 1–6, 2017. 2, 5, 6, 7, 8, 12
- [12] D. Cozzolino and L. Verdoliva. Noiseprint: a CNN-based camera model fingerprint. *arXiv:1808.08396*, 2018. 3
- [13] G. Csurka. *A Comprehensive Survey on Domain Adaptation for Visual Applications*, pages 1–35. Springer International Publishing, 2017. 3
- [14] T. de Carvalho, C. Riess, E. Angelopoulou, H. Pedrini, and A. Rocha. Exposing digital image forgeries by illumination color classification. *IEEE Transactions on Information Forensics and Security*, 8(7):1182–1194, 2013. 2
- [15] H. Farid. *Photo Forensics*. The MIT Press, 2016. 1
- [16] P. Ferrara, T. Bianchi, A. D. Rosa, and A. Piva. Image Forgery Localization via Fine-Grained Analysis of CFA Artifacts. *IEEE Transactions on Information Forensics and Security*, 7(5):1566–1577, Oct 2012. 2
- [17] X. Glorot, A. Bordes, and Y. Bengio. Domain adaptation for large-scale sentiment classification: A deep learning approach. In *International Conference on Machine Learning*, pages 513–520, 2011. 3
- [18] I. Goodfellow, J. Pouget-Abadie, M. Mirza, B. Xu, D. Warde-Farley, S. Ozair, A. Courville, and Y. Bengio. Generative adversarial nets. In *Advances in neural information processing systems*, pages 2672–2680, 2014. 3
- [19] J. Hoffman, E. Tzeng, T. Park, J.-Y. Zhu, P. Isola, K. Saenko, A. A. Efros, and T. Darrell. Cycada: Cycle-consistent adversarial domain adaptation. *arXiv preprint arXiv:1711.03213*, 2017. 3
- [20] M. Huh, A. Liu, A. Owens, and A. Efros. Fighting fake news: Image splice detection via learned self-consistency. In *European Conference on Computer Vision (ECCV)*, 2018. 3
- [21] S. Iizuka, E. Simo-Serra, and H. Ishikawa. Globally and Locally Consistent Image Completion. *ACM Transactions on Graphics (Proc. of SIGGRAPH 2017)*, 36(4):107:1–107:14, 2017. 2, 6, 7, 8, 11
- [22] T. Karras, T. Aila, S. Laine, and J. Lehtinen. Progressive Growing of GANs for Improved Quality, Stability, and Variation. In *International Conference on Learning Representations*, 2018. 2, 6, 7, 8
- [23] H. Kim, P. Garrido, A. Tewari, W. Xu, J. T. M. Nießner, P. Pérez, C. Richardt, M. Zollhöfer, and C. Theobalt. Deep Video Portraits. *ACM Transactions on Graphics (TOG)*, 2018. 2

- [24] D. Kingma and P. Dhariwal. Glow: Generative flow with invertible 1x1 convolutions. *arXiv preprint arXiv:1807.03039*, 2018. [2](#), [6](#), [8](#), [11](#)
- [25] E. Kodirov, T. Xiang, and S. Gong. Semantic autoencoder for zero-shot learning. In *IEEE Conference on Computer Vision and Pattern Recognition*, pages 4447–4456, 2017. [3](#)
- [26] X. Liang, H. Zhang, L. Lin, and E. Xing. Generative semantic manipulation with mask-contrasting gan. In *European Computer Vision Conference (ECCV)*, 2018. [2](#)
- [27] Y. Liu, Q. Guan, X. Zhao, and Y. Cao. Image forgery localization based on multi-scale convolutional neural networks. In *ACM Workshop on Information Hiding and Multimedia Security*, 2018. [2](#)
- [28] Z. Liu, P. Luo, X. Wang, and X. Tang. Deep learning face attributes in the wild. In *IEEE International Conference on Computer Vision (ICCV)*, pages 3730–3738, 2015. [6](#)
- [29] S. Lyu, X. Pan, and X. Zhang. Exposing region splicing forgeries with blind local noise estimation. *International Journal of Computer Vision*, 110(2):202–221, 2014. [2](#)
- [30] F. Marra, D. Gragnaniello, D. Cozzolino, and L. Verdoliva. Detection of GAN-Generated Fake Images over Social Networks. In *IEEE Conference on Multimedia Information Processing and Retrieval*, pages 384–389, 2018. [3](#)
- [31] A. Pumarola, A. Agudo, A. Martinez, A. Sanfeliu, and F. Moreno-Noguer. GANimation: Anatomically-aware Facial Animation from a Single Image. In *European Conference on Computer Vision (ECCV)*, 2018. [2](#)
- [32] N. Rahmouni, V. Nozick, J. Yamagishi, and I. Echizeny. Distinguishing computer graphics from natural images using convolution neural networks. In *IEEE Workshop on Information Forensics and Security*, pages 1–6, 2017. [2](#), [7](#), [8](#), [12](#)
- [33] Y. Rao and J. Ni. A deep learning approach to detection of splicing and copy-move forgeries in images. In *IEEE International Workshop on Information Forensics and Security (WIFS)*, pages 1–6, 2016. [2](#)
- [34] A. Rössler, D. Cozzolino, L. Verdoliva, C. Riess, J. Thies, and M. Nießner. Faceforensics: A large-scale video dataset for forgery detection in human faces. *arXiv preprint arXiv:1803.09179*, 2018. [2](#), [6](#), [7](#)
- [35] O. Russakovsky, J. Deng, H. Su, J. Krause, S. Satheesh, S. Ma, Z. Huang, A. Karpathy, A. Khosla, M. Bernstein, A. C. Berg, and L. Fei-Fei. ImageNet Large Scale Visual Recognition Challenge. *International Journal of Computer Vision*, 115(3):211–252, Dec 2015. [6](#), [7](#)
- [36] R. Salloum, Y. Ren, and C. C. J. Kuo. Image Splicing Localization using a Multi-task Fully Convolutional Network (MFCN). *Journal of Visual Communication and Image Representation*, 51:201–209, 2018. [2](#)
- [37] S. Suwajanakorn, S. M. Seitz, and I. Kemelmacher-Shlizerman. Synthesizing Obama: learning lip sync from audio. *ACM Transactions on Graphics (TOG)*, 36(4):95, 2017. [2](#)
- [38] C. Szegedy, W. Liu, Y. Jia, P. Sermanet, S. Reed, D. Anguelov, D. Erhan, V. Vanhoucke, and A. Rabinovich. Going deeper with convolutions. In *IEEE Conference on Computer Vision and Pattern Recognition (CVPR)*, pages 1–9, June 2015. [7](#)
- [39] J. Thies, M. Zollhöfer, M. Stamminger, C. Theobalt, and M. Nießner. Face2Face: Real-Time Face Capture and Reenactment of RGB Videos. In *IEEE Conference on Computer Vision and Pattern Recognition (CVPR)*, pages 2387–2395, June 2016. [2](#), [3](#), [5](#), [6](#), [7](#), [8](#)
- [40] E. Tzeng, J. Hoffman, K. Saenko, and T. Darrell. Adversarial discriminative domain adaptation. In *IEEE Conference on Computer Vision and Pattern Recognition (CVPR)*, volume 1, page 4, 2017. [3](#)
- [41] I. Yerushalmy and H. Hel-Or. Digital image forgery detection based on lens and sensor aberration. *International Journal of Computer Vision*, 92(1):71–91, 2018. [2](#)
- [42] J. Yu, Z. Lin, J. Yang, X. Shen, X. Lu, and T. S. Huang. Generative image inpainting with contextual attention. In *IEEE Conference on Computer Vision and Pattern Recognition (CVPR)*, 2018. [6](#), [7](#), [8](#), [11](#)
- [43] B. Zhou, A. Khosla, A. Lapedriza, A. Oliva, and A. Torralba. Learning deep features for discriminative localization. In *IEEE Conference on Computer Vision and Pattern Recognition (CVPR)*, pages 2921–2929, 2016. [4](#)
- [44] P. Zhou, X. Han, V. Morariu, and L. Davis. Learning rich features for image manipulation detection. In *IEEE Conference on Computer Vision and Pattern Recognition (CVPR)*, 2018. [2](#)
- [45] J. Zhu, T. Park, P. Isola, and A. Efros. Unpaired image-to-image translation using cycle-consistent adversarial networks. In *IEEE International Conference on Computer Vision (ICCV)*, 2017. [2](#), [6](#), [7](#), [8](#), [11](#)
- [46] J.-Y. Zhu, P. Krähenbühl, E. Shechtman, and A. Efros. Learning a Discriminative Model for the Perception of Realism in Composite Images. In *IEEE International Conference on Computer Vision (ICCV)*, 2015. [2](#)

## ForensicTransfer — Supplemental Document

*ForensicTransfer* shows state-of-the-art results on the transferability of forgery detection. Given a database of manipulated images from a source domain, we are able to detect fakes generated with a different manipulation method (target domain). In this supplemental document, we report additional experiments that confirm the potential of the proposed forensic embedding. We first analyze the influence of having multiple source domains to the detectability of fakes in a target domain (see Sec. A). In a second experiment, we show the impact of the dimension of the forensic embedding (see Sec. B). Finally, we give a conclusion.

### A. Multi-source experiments

In the main paper we are showing examples of a one-to-one transferability of forgery detection. Given multiple source domains, we can extend this idea to a many-to-one transfer of knowledge. To this end, we train the network proposed in the main paper on a dataset of multiple sources. Specifically, we use the following methods for our experiment (see Fig. 10). As source domain we generate images using StarGAN [9] and Glow [24]. The target domain images are synthesized by a CycleGAN [45]. Based on the images of the two source domains, we train the encoder-decoder network, disentangling the knowledge about real and fake images. In Tab. 2 we show the zero-shot results in comparison to a one-to-one transfer. The multi-source training helps to detect unknown forgeries in the target domain by at least 7% in terms of accuracy. To compare the few-shot adaptation w.r.t. the baseline methods presented in the main paper, we included Fig. 11 in this document. All methods are trained on both source domains. As can be seen our approach behaves similarly to the one-to-one experiments conducted in the main paper. Our approach outperforms all baselines, especially, when there are less than 5 target domain samples available by more than 25%.

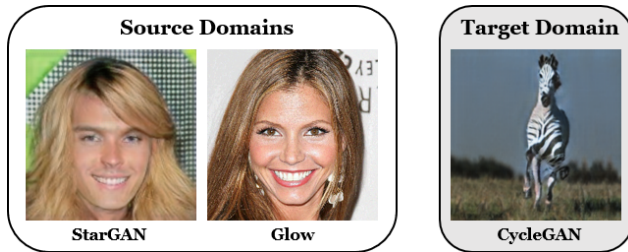


Figure 10: Samples of our three methods generating synthetic images. StarGAN [9] and Glow [24] images are used as source domain, while CycleGAN [45] is used as target domain method.

### B. Dimensionality of the Forensic Embedding

In this section, we evaluate the influence of the dimensionality of the forensic embedding. The results reported in the main paper are based on a forensic embedding of size 128. Where we are using 64 to encode pristine and another 64 to encode manipulated images. In this experiment, we reduce and increase the number of features in the latent space. Tab. 3 shows the zero-shot performance for a one-to-one transfer on the inpainting dataset (Iizuka et al. [21] as source and Yu et al. [42] as target domain. As can be seen the dimensionality has an influence on the performance and 128 is the sweet spot with the best performance. With a lower or higher dimensionality of the feature space, the transferability performance decreases, but is still better or comparable with respect to the baseline methods.

The few-shot adaptation experiment in Fig. 12 shows that the performance of the 128 long feature space is consistently better than the other configurations while they converge with the number of samples from the target domain.

	Accuracy
one-to-one (Pro.GAN)	85.00
one-to-one (StarGAN)	77.26
one-to-one (Glow)	83.67
multi-to-one (StarGAN+Glow)	<b>92.32</b>

Table 2: Our approach enables the transfer of detection abilities from multiple source domains to a target domain. Here, we show zero-shot results using our approach based on a one-to-one transfer in comparison to a multi-to-one transfer. The target domain is composed by images generated with CycleGAN, while the source domain is different (Pro.GAN, StarGAN, and Glow).

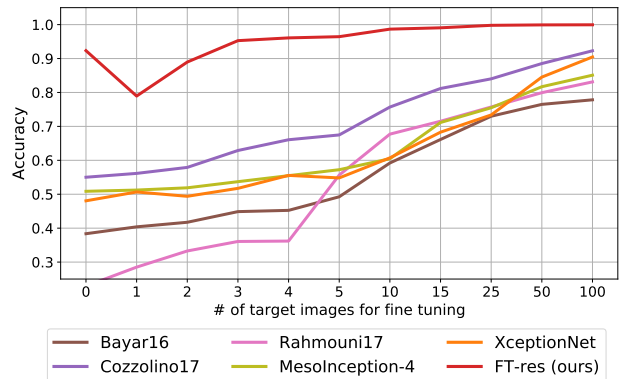


Figure 11: Few-shot adaptation experiment in a multi-to-one transfer scenario. Plots show accuracy versus number of images used for fine-tuning (shots). Values are averaged over 10 runs.

	Accuracy
Bayar16 [7]	50.10
XceptionNet [10]	51.08
Rahmouni17 [32]	52.02
Cozzolino17 [11]	63.33
MesoInception-4 [3]	67.30
Ours (32)	56.32
Ours (64)	64.60
Ours (128)	<b>70.62</b>
Ours (256)	62.17
Ours (512)	59.75

Table 3: Here, we show an ablative study regarding the dimension of the forensic embedding. The results are based on a zero-shot one-to-one transfer scenario.

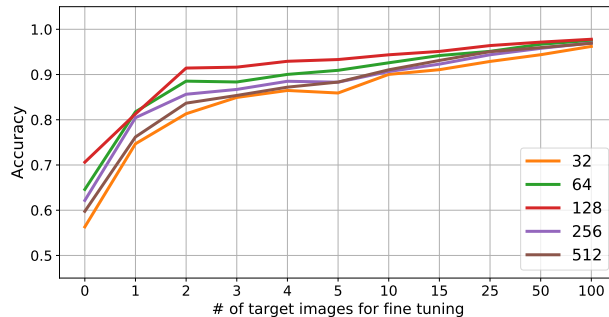


Figure 12: In this graph, we show the few-shot adaptation abilities with different dimensions of the forensic embedding. Plots show accuracy versus number of images used for fine-tuning (shots). Values are averaged over 10 runs.

### C. Conclusion

*ForensicTransfer* is able to transfer the ability of detecting forgeries from one domain to another. In this supplemental document, we also show that one can use multiple source domains to improve the detection performance on a target domain. We think this is a stepping stone towards general approaches for forgery detection, where samples of existing methods can be used to train a detector that can be used to unmask novel manipulation techniques.